

where

$$F(a) = \int_0^{\infty} (1+y)^{-2} \cos ay dy, \quad a = RE_{\gamma}/hc\beta,$$

β is the deuteron velocity divided by the velocity of light and σ_d is the known cross section for the photo-disintegration of the deuteron as a function of photon energy E_{γ} . Evaluating this expression for a 6-MeV deuteron emerging from copper gives the probability of breaking apart to be small. This is in agreement with a recent calculation by Gold and Wong.²⁷ We conclude, then, that the deuteron is not usually available for evaporation and probably does not exist with appreciable probability in the preformed condition in the copper nucleus.

The amount of deuterium observed from copper with 40-MeV bremsstrahlung, giving a deuterium to hydrogen ratio of approximately 0.0009 is not too far from the 0.0012 predicted by the two stage direct interaction for high residual nucleus excitation. An uncertainty of a factor of two probably should be allowed in each number.

²⁷ R. Gold and C. Wong, Phys. Rev. (to be published).

TABLE VIII. Comparison of deuteron to proton yield ratios for various evaporation models with observed values.

Maximum bremsstrahlung energy	Theoretical ratios	Observed ratios
24 MeV	0.00027 to 0.0069	<0.0016
30 MeV	0.0046 to 0.090	<0.0014
40 MeV	0.019 to 0.266	~0.0009

The experimental upper limit of the ratio at 30 MeV is somewhat lower than the direct interaction picture predicts. However, since this is closer to the thresholds, more uncertainty may accrue to the rough calculations. The experimental results may then be regarded as consistent with the Madsen and Henley theory if the residual nucleus is left in states of relatively high excitation (possibly because of picking up the particle from a closed shell).

This seems equivalent to the conclusions of Chizhov *et al.*⁹ that the direct pickup process is verified and that the residual nucleus must be left with sufficient energy to separate a further nucleon.

Inelastic Proton Scattering from Nuclei with 28 Neutrons*

H. O. FUNSTEN,[†] N. R. ROBERSON,[‡] AND E. ROST

Palmer Physical Laboratory, Princeton University, Princeton, New Jersey

(Received 9 October 1963; revised manuscript received 30 December 1963)

The inelastic scattering of 17.45-MeV protons from Ti^{50} , Cr^{52} , Fe^{54} , and V^{51} has been measured. Levels up to 5-MeV excitation were studied and the 30° - 90° differential cross sections were measured for most of the levels. Spins and parities were assigned on the basis of the angular distributions and agree well with other experiments. The strength of the various inelastic cross sections were studied using a direct reaction theory with distorted waves. Both the collective model and the shell model of nuclear structure were used to describe the nuclear states. In describing the excitation of the strongly excited levels of the even- A nuclei, the collective model picture yielded a strength parameter, β_1 , which agreed within experimental error with the β_1 value extracted from Coulomb excitation experiments. The shell-model formulation described this data as well using a two-body Gaussian potential of finite range and depth of 45 MeV. The analysis of V^{51} , however, was better explained using a shell-model analysis.

I. INTRODUCTION

INELASTIC proton scattering has been a useful technique for investigating the level structure of nuclei. For bombarding energies in the range $10 < E_p < 20$ MeV, the inelastic scattering from nuclei with $A > 40$ does not usually depend sensitively on energy, and the direct process as opposed to compound nuclear formation seems to be predominant in exciting low-lying

($\lesssim 5$ MeV) states.¹ Furthermore, recent developments in theoretical techniques² have greatly simplified the extraction of nuclear structure information from the experimental data.

The inelastic scattering reaction has been formulated using either collective-model or shell-model wave functions to describe the nuclear states. The collective-model treatment has been very successful in the

* This work was supported by the U. S. Atomic Energy Commission and the Higgins Scientific Trust Fund.

[†] Present address: The Department of Physics, College of William and Mary, Williamsburg, Virginia.

[‡] Present address: The Department of Physics, Duke University, Durham, North Carolina.

¹ G. Schrank, E. K. Warburton, and W. W. Daehnick, Phys. Rev. **127**, 2159 (1962).

² R. H. Bassel, R. H. Drisko, and G. R. Satchler, Oak Ridge National Laboratory Report ORNL-3240, 1962 (unpublished).

description of (α, α') reactions.³⁻⁵ In addition, experimental⁶ and theoretical⁷ evidence points to a strong correlation between the excitation of low-lying levels by inelastic scattering and by electromagnetic means. Since the latter are known to be dominated by collective effects⁸ it is certainly reasonable to use a collective-model analysis of inelastic scattering.

The shell-model treatment of inelastic scattering requires a more complete description of the reaction than the usual collective-model treatment. Thus it is possible, in principle, to extract more detailed nuclear structure information by using the shell-model picture. Previous shell-model analyses⁹ of (p, p') have dealt with light nuclei and have met difficulties in explaining the absolute magnitude of the cross section. These difficulties may not be as serious for heavier nuclei.¹⁰

A convenient group of nuclei to study (p, p') reactions are the isotones with $N=28$, viz., ${}_{22}\text{Ti}^{50}$, ${}_{23}\text{V}^{51}$, ${}_{24}\text{Cr}^{52}$, and ${}_{26}\text{Fe}^{54}$. For these nuclei the proton $1f_{7/2}$ subshell is being filled and is well separated in energy from other subshells. Consequently, a $(1f_{7/2})^n$ proton configuration is a reasonable wave function with which to describe low-lying nuclear states.

This paper reports the results of measurements of the excitation of low-lying levels of Ti^{50} , Cr^{52} , Fe^{54} , and V^{51} by the inelastic scattering of 17.45-MeV protons. The results of both a shell-model and a collective-model analysis of the data will be presented using distorted waves. Comparison will also be made with the results of other experiments, especially Coulomb excitation.

II. EXPERIMENTAL PROCEDURE

The experimental arrangement is shown in Fig. 1. The external proton beam from the Princeton FM cyclotron was focused on the entrance slit of a double-focusing magnetic spectrometer by two pairs of wedge-shaped magnets and a uniform-field bending magnet. The double-focusing spectrometer slits were adjusted so that a beam current of 3×10^{-9} A could be maintained with an energy spread of 30 keV. The magnet was calibrated using the limp-wire technique to an accuracy of 50 keV.¹¹ All measurements reported here were done with a proton energy of 17.45 ± 0.05 MeV. The experi-

ments were carried out in a 20-in. scattering chamber designed for use with solid-state detectors.¹²

The scattered protons were detected by 2.5-mm-thick Li-drift junction detectors.¹³ The intrinsic noise at room temperature for these detectors was 50 to 70 keV. It has been observed in several laboratories that the energy resolution can be improved by operating Li-drift detectors at low temperature.^{14,15} The detectors were mounted on thermoelectric coolers¹⁶ which cooled them to 0°C. The noise observed after cooling to 0°C was usually 30-keV full width at half-maximum. To protect the Li surface from pump-oil vapor, each counter was mounted in an Al block and a snout was fitted to the front of the counter. The snout was closed with a $\frac{1}{4}$ -mil Mylar window. To allow pump-out, a small curved copper tube was soldered to the side of the snout. The whole assembly is thus cooled and very little oil reaches the Li surface. Low-noise ORTEC amplifying systems¹⁷ were used to amplify the signals. Three detectors were operated simultaneously and were mounted at 20° intervals on the scattering table. The counter at the smallest scattering angle was fed into a RIDL 400-channel pulse analyzer, while the output of the other two counters were mixed and fed into a Nuclear Data 1024-channel analyzer. The mixing was done in a simple resistor network following the ORTEC post-amplifiers so that detector noise was not summed. A routing signal caused the pulses from the detector at the largest scattering angle to be stored in the upper 512 channels of the memory. The over-all energy resolution was 85 to 90 keV. This is larger by 20 to 30 keV than was expected from the known beam spread, detector-amplifier noise, and target thickness. Furthermore, the shapes of the peaks in our spectra were not Gaussian and were, in fact, different for each individual detector. These effects were investigated by using 5.3-MeV incident alpha particles. The same line shape was observed as with protons but with a width of several hundred keV. By calculating the equivalent proton energy losses in Li, an increase in peak width of about 20 to 30 keV for protons is expected. Therefore, the poorer resolution and non-Gaussian line shape can be attributed to an uneven Li layer on the faces of the detectors.

The targets used were self-supporting metal foils of about 1 mg/cm². The Ti^{50} and Fe^{54} targets were enriched isotopic foils (69.7% and 95.3% purity, respectively), while the V and Cr targets were natural (99.75% V^{51} and 83.7% Cr^{52}). The Fe^{54} foil was very nonuniform, so the absolute cross section was determined by suspending $\text{Fe}_2^{54}\text{O}_3$ in polystyrene and com-

³ J. S. Blair, Phys. Rev. **115**, 928 (1959).

⁴ E. Rost and N. Austern, Phys. Rev. **120**, 1375 (1960).

⁵ R. H. Bassel, G. R. Satchler, R. M. Drisko, and E. Rost, Phys. Rev. **128**, 2693 (1962).

⁶ B. L. Cohen and A. G. Rubin, Phys. Rev. **111**, 1568 (1958).

⁷ W. T. Pinkston and G. R. Satchler, Nucl. Phys. **27**, 270 (1961).

⁸ K. Alder, A. Bohr, T. Huus, B. Mottelson, and A. Winther, Rev. Mod. Phys. **28**, 432 (1956).

⁹ C. A. Levinson and M. K. Banerjee, Ann. Phys. (N. Y.) **2**, 471 (1957); E. Rost, University of Pittsburgh, Ph.D. thesis, 1961 (unpublished).

¹⁰ An indication of the promise of a distorted-wave analysis in this mass region was given by the excellent agreement between sample calculations [Satchler (unpublished)] and Princeton data [$\text{Ni}^{58}(p, p')$; H. A. Hill and R. Sherr, Bull. Am. Phys. Soc. **5**, 249 (1960) and W. W. Daehnick (unpublished)].

¹¹ We wish to thank Dr. R. E. Pollock for making this measurement.

¹² A. Lieber (to be published).

¹³ R. C. A. Victor Company, Montreal, Canada.

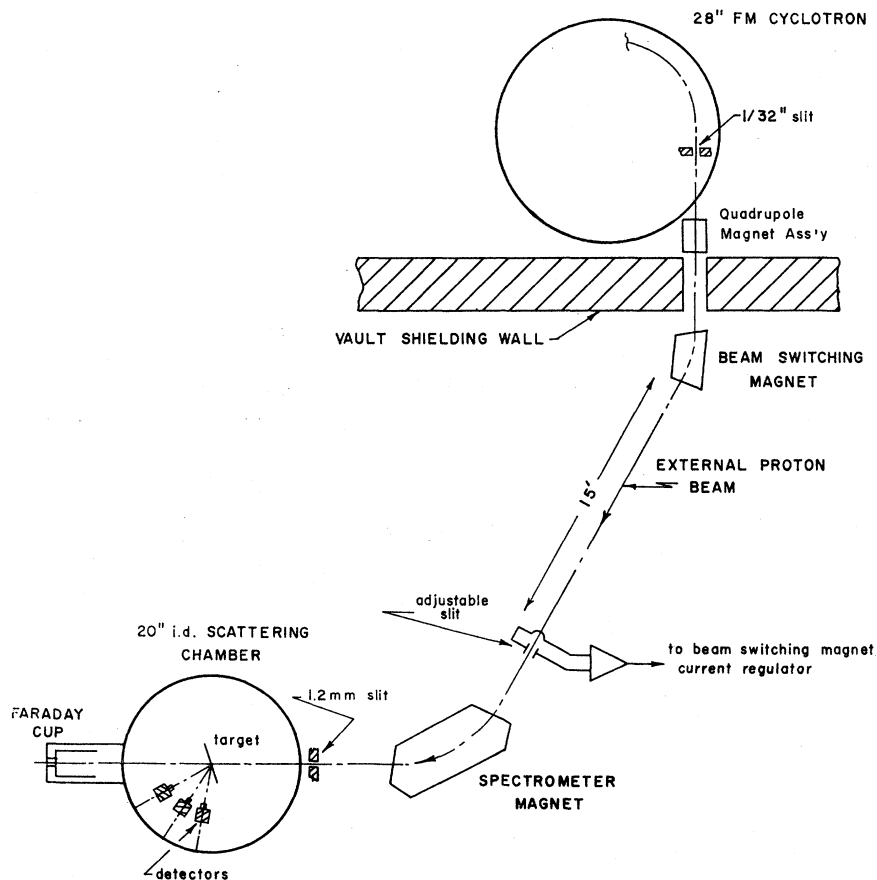
¹⁴ H. M. Mann, J. W. Haslett, and F. J. Janauh, IRE Trans. NS-9, No. 4, 43 (1962).

¹⁵ J. L. Blankenship and C. J. Borkowsky, IRE Trans. NS-9, No. 3, 181 (1962).

¹⁶ Neeco Frigistors, Montreal, Canada.

¹⁷ ORTEC Model 203, Oak Ridge, Tennessee.

FIG. 1. Cyclotron external beam system.



paring the absolute scattering from Fe^{54} with an accurate $\text{O}^{16}(p,p)\text{O}^{16}$ measurement of Daehnick and Sherr.¹⁸ We checked this technique by comparing a $\text{Fe}_2^{56}\text{O}_3$ target with the elastic proton scattering measurements of Dayton and Schrank.¹⁹ The agreement was within the statistical accuracy of the two sets of data. The Ti^{50} , Cr^{52} , and V^{51} cross sections were determined from the weight of the foils. The absolute cross sections of the ground states are estimated to be correct to within 10%. The errors for the excited states are usually determined by the statistics and by uncertainty in background subtraction. Oxygen and carbon were present as a contamination in all four targets, but could be easily subtracted out by using the known O^{16} or C^{12} differential cross section. Other reaction particles may appear as peaks but can usually be identified by line shape and from kinematics.

The energies of the excited states were determined by comparison with the known levels of C^{12} and O^{16} . Relative errors of the excitation energies are about 30 keV, and for known levels there are no systematic deviations. After the levels were identified and other background subtracted, the inelastic cross sections were obtained

by comparison of the ground-state peaks to the levels in question. In all cases, levels up to 6-MeV excitation had the same shape as the ground state peaks.

III. THE DISTORTED-WAVE THEORY

The distorted-wave (DW) theory for inelastic scattering has been formulated elsewhere² so that only the pertinent formulas will be listed for identification purposes. The differential cross section for exciting the target nucleus from a state $|i\rangle$ to a final state $|f\rangle$ is

$$\frac{d\sigma}{d\Omega} = \frac{k_f}{k_i} \left(\frac{m}{2\pi\hbar^2} \right)^2 \sum_{AV} |T_{fi}|^2, \quad (1)$$

$$T_{fi} = \int d\mathbf{r} \chi_f^{(-)*}(\mathbf{k}_f, \mathbf{r}) \langle f | V | i \rangle \chi_i^{(+)}(\mathbf{k}_i, \mathbf{r}). \quad (2)$$

Here m is the reduced mass of the colliding pair, $\hbar\mathbf{k}_i$ and $\hbar\mathbf{k}_f$ their relative momenta in initial and final channels, respectively, and $\chi_i^{(+)}$ and $\chi_f^{(-)}$ the distorted-wave functions of relative motion satisfying

$$[-(\hbar^2/2m)\nabla^2 + U(r) - E]\chi = 0 \quad (3)$$

with appropriate boundary conditions. The optical potential, $U(r)$, is that which reproduces the elastic

¹⁸ W. W. Daehnick and R. Sherr, Phys. Rev. **133**, B934 (1964).

¹⁹ I. E. Dayton and G. Schrank, Phys. Rev. **101**, 1358 (1956).

scattering at the incident energy and is assumed to be spin-independent. Exchange effects due to antisymmetrization are also ignored.

The interaction V is assumed to be static and non-exchange. Expanding into multipoles and applying the Wigner-Eckart theorem allows us to write the matrix element in (2) as

$$\langle v_f J_f M_f | V | v_i J_i M_i \rangle = \sum_{lm} (l J_i m M_i | J_f M_f) F_l(r) [i^l Y_l^m(r)]^*, \quad (4)$$

where $F_l(r)$ is our notation for the reduced matrix element and will be often called a form factor. This function vanishes exponentially at large radii and in general peaks in the region of the nuclear "surface." The extra quantum numbers necessary to completely specify to nuclear states are denoted by v (e.g., seniority). Substituting (4) into (2) and performing the sums in (1) yields

$$\frac{d\sigma}{d\Omega} = \frac{k_f}{k_i} \left(\frac{m}{2\pi\hbar^2} \right)^2 \frac{2J_f+1}{2J_i+1} \sum_{lm} |B^{lm}|^2, \quad (5)$$

$$B^{lm} = (2l+1)^{-1/2} \int d\mathbf{r} \chi_{f^{(-)*}}(\mathbf{k}_f, \mathbf{r}) F_l(r) \times [i^l Y_l^m(\hat{r})]^* \chi_{i^{(+)}}(\mathbf{k}_i, \mathbf{r}). \quad (6)$$

The expressions (5) and (6) are easily evaluated using the Oak Ridge computer program SALLY.²

A. Collective Excitation

A simple model which describes inelastic scattering may be derived from a deformed, or nonspherical potential well. Let us assume a potential of the form

$$U = U(r - R(\theta')), \quad R(\theta') = R_0 [1 + \sum_l \beta_l Y_l^0(\theta')], \quad (7)$$

where θ' is measured in the body-fixed frame. We expand U in powers of β_l identifying the β_l -independent (i.e., spherical) term as the distorting optical potential. Treating the first-order term as the interaction and using (4) gives

$$F_l(r) = -(2l+1)^{-1/2} \beta_l R_0 (d/dr) U(r), \quad (8)$$

which may be put into (6) and evaluated using SALLY. For an even-even target, $J_i=0$, so that only a single $l=J_f$ is allowed and a single parameter β_l^2 is extracted. This parameter is related to the restoring-force parameter, C_l , of the first-order vibrational model by

$$\beta_l^2 = (2l+1) (\hbar\omega_l / 2C_l),$$

where $\hbar\omega_l$ is the energy of the excited state.

B. Single-Particle Excitation

The shell-model approach to inelastic scattering assumes the interaction V to be a sum of central

two-body potentials

$$V = \sum_{j=1}^n V(|\mathbf{r} - \mathbf{r}_j|).$$

A particularly convenient form for the potentials is the Gaussian because of its multipole expansion

$$V_G e^{-\gamma^2(r-r_j)^2} = 4\pi V_G \sum_{\lambda\mu} i^\lambda j_\lambda(-2i\gamma^2 r r_j) \times e^{-\gamma^2(r^2+r_j^2)} Y_{\lambda\mu}(\hat{r}_j) Y_{\lambda\mu}^*(\hat{r}). \quad (9)$$

The nuclear states we consider are described by a single n -particle configuration. The form factor is then easily obtained using Eq. (4) and may be written as

$$F_l(r) = 4\pi V_G M_l I_l(r), \quad (10)$$

$$M_l = \sum_{\mu M_i} (l J_i \mu M_i | J_f M_f) \langle v_f J_f M_f | \sum_{j=1}^n Y_l^\mu(\hat{r}_j) | v_i J_i M_i \rangle, \quad (11)$$

$$I_l(r) = e^{-\gamma^2 r^2} (-1)^l \int r_j^2 dr_j j_l(-2i\gamma^2 r r_j) e^{-\gamma^2 r_j^2} [u(r_j)]^2. \quad (12)$$

It should be noted that $I_l(r)$ depends on the nuclear structure only through the orbital wave function $u(r_j)$ and thus is rather constant for neighboring nuclei in the same shell. The angular matrix element, however, is quite sensitive to the number of particles and also to the coupling scheme.

C. Choice of Parameters

The optical parameters for all the distorted-wave calculations have been taken from a systematic optical-model analysis by Perey.²⁰

$$-V_s f(r, r_{0R}, a_R) + i a_I W_D (d/dr) f(r, r_{0I}, a_I) + V_{\text{Coul}} f(r, r_0, a) = \{1 + \exp[(r - r_0 A^{1/3})/a]\}^{-1} \quad V_{\text{Coul}} = (Z e^2 / 2R_c) (3 - r^2 / R_c^2), \quad r \leq R_c \quad (13) \\ = Z e^2 / r, \quad r > R_c$$

with $V_s = 48$ MeV, $r_{0R} = r_{0I} = 1.25$, $W_D = 44$ MeV, $a_R = 0.65$, $a_I = 0.47$ and $R_c = 1.25 A^{1/3}$. For simplicity we ignore the spin-orbit potential since we have found that its inclusion makes little difference. We also use the same parameters for the final channel and for all four nuclei studied. The agreement with elastic-scattering data is excellent.

In applying the collective model to the analysis of (p, p') , we assume that $U(r)$ in Eq. (8) is the real part of the optical potential. The cross section is now calculable up to a β_l^2 normalization constant and is presented in Fig. 2 for $\text{Cr}^{52}(p, p')\text{Cr}^{52*}$ for $l=2, 3$, and 4 , assuming an energy loss, $Q = -1.0, -4.0$, and -2.5 MeV, respectively. The dependence on Q and A for the cases described in this paper is quite unimportant.

For the shell-model DW calculations, we use a two-body Gaussian which fits the 1S_0 nucleon-nucleon effec-

²⁰ F. G. Perey, Phys. Rev. **131**, 745 (1963).

tive range. This yields $\gamma=0.561f^{-1}$. The orbital wave function required in (12) is obtained by solving the Schrödinger equation in a Saxon well of form $47.5[1+\exp(r_j-1.29A^{1/3}/0.65)]^{-1}$ MeV for a $1f$ orbital. The binding energy eigenvalue obtained is 8.3 MeV. This orbital wave function $u(r_j)$ is assumed to be applicable to all the levels analyzed in this paper.

The integrals $I_i(r)$ in (12) were evaluated by computer and then used in SALLY giving the "universal curves" plotted in Fig. 3. The σ_i curves are normalized so that the cross section for exciting a level of spin J_f with target spin J_i is

$$\frac{d\sigma}{d\Omega}(\theta) = \frac{2J_f+1}{2J_i+1} V_G^2 \sum_i \frac{M_i^2}{2l+1} \sigma_l(\theta) \frac{\text{mb}}{\text{sr}}. \quad (14)$$

It should be noted that the shapes of the σ_l curves are almost identical with the shapes of the collective-model curves in Fig. 2.

The angular matrix elements are conveniently obtained by using a fractional-parentage decomposition.²¹

TABLE I. Square of angular matrix element M_l^2 (see text) for nuclei with 28 neutrons.

Ti ⁵⁰ or Fe ⁵⁴		Cr ⁵²	
l		($v=2$)	($v=4$)
2	0.0758	0.101	0
4	0.0372	0.0495	0
6	0.0185	0.0248	0

		V ⁵¹				
$l \setminus J_f$		3/2	5/2	9/2	11/2	15/2
2	0.065	0.185	0.0313	0.0842	0	
4	0.117	0.009	0.0966	0.0293	0.0338	
6	0	0.024	0.0184	0.0390	0.0573	

For the cases considered in this paper we have a simple j^n configuration and thus can write for the matrix element

$$M_l = n \sum_{vK} (-1)^{J_f-J_i} (j^{n-1}vK; j | j^n v_i J_i) \times (j^{n-1}vK; j | j^n v_f J_f) U(ljJ_fK; jJ_i) \times (lj0\frac{1}{2} | j\frac{1}{2}) \left[\frac{2l+1}{4\pi} \right]^{1/2}. \quad (15)$$

The extra quantum numbers v_i and v_f are needed only for Cr⁵² in which case we assume that the ground state is seniority 0 and the excited states, seniority 2 or 4. In Table I, values are listed for the squares of the angular matrix elements for the nuclei studied. These values may then be inserted into (14) and the strength parameter V_G may be extracted from the data in a manner analogous to the extraction of β_l using the collective model.

²¹ A. R. Edmonds and B. H. Flowers, Proc. Roy. Soc. (London) **A214**, 515 (1952).

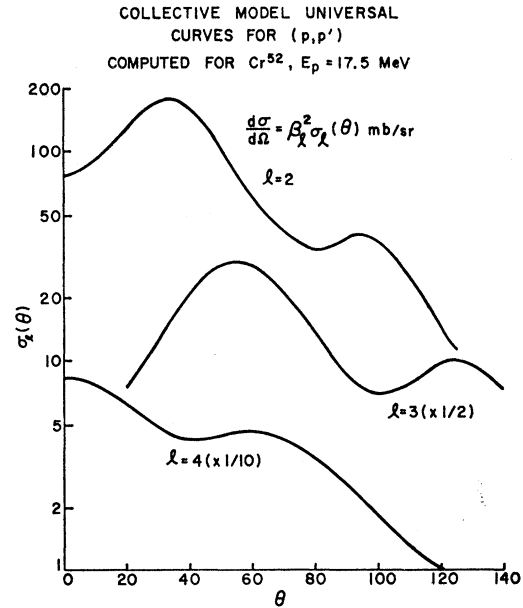


Fig. 2. Theoretical distorted-wave angular distributions based on the collective model. The Q values used were -1.0 , -2.5 , and -4.0 MeV for $l=2, 4$, and 3 , respectively. The optical parameters are given in the text.

IV. EXPERIMENTAL RESULTS

A. Fe⁵⁴

An energy spectrum of protons scattered from Fe⁵⁴ is shown in Fig. 4 for a laboratory angle of 54.5 deg.

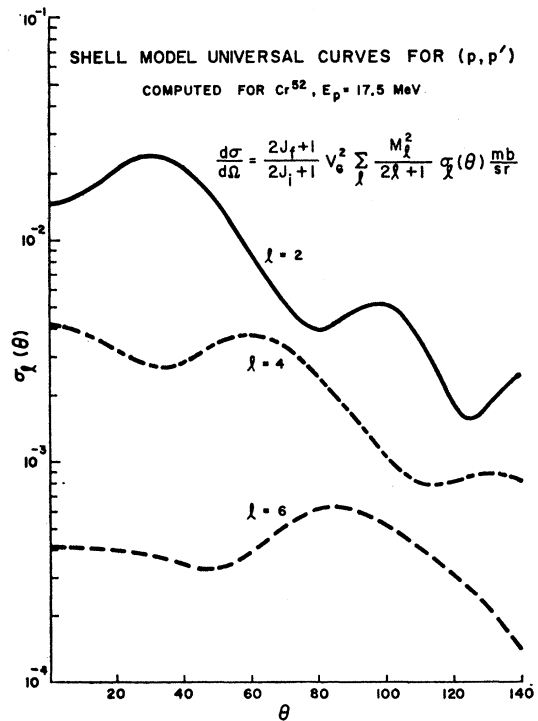


Fig. 3. Theoretical distorted-wave angular distributions based on the shell model (see text). The Q value was -1.0 MeV. The parameters used are given in the text.

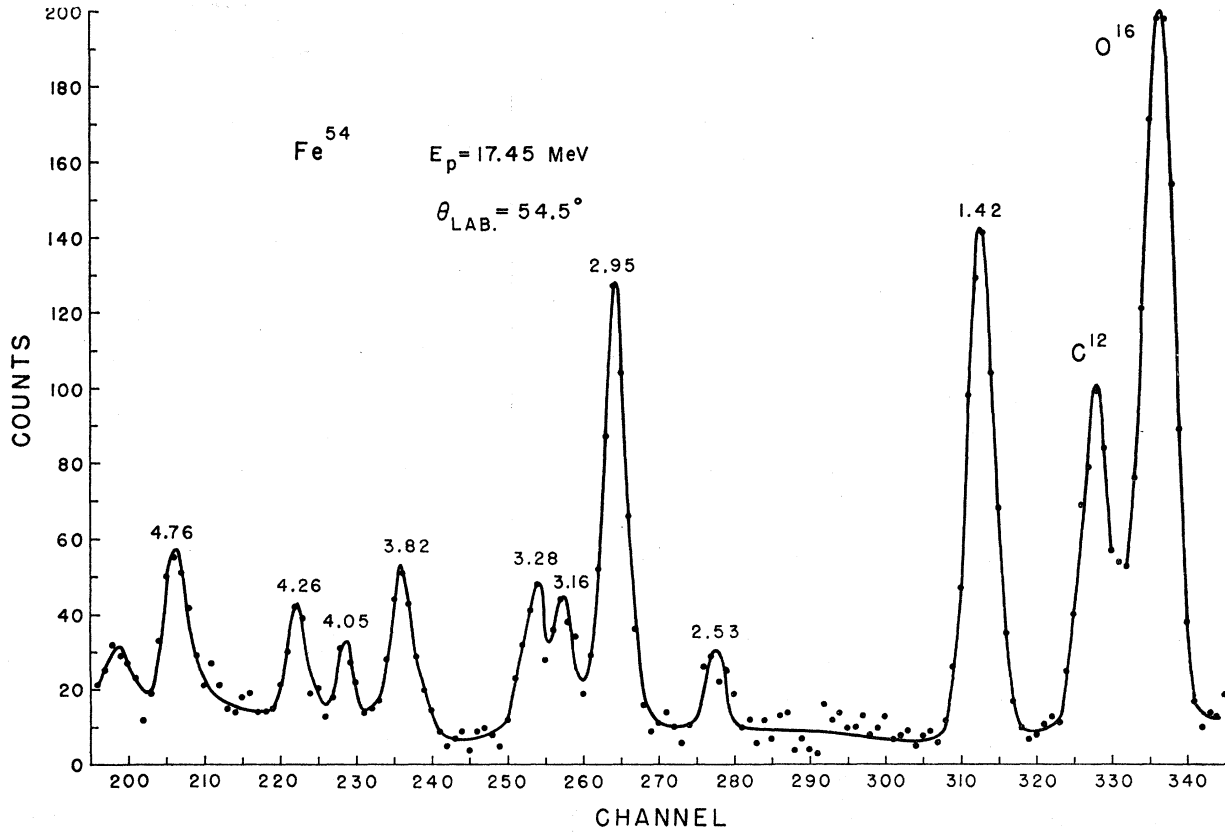


FIG. 4. Energy spectra of protons scattered from Fe^{54} . The curve is a smooth line drawn through the experimental points.

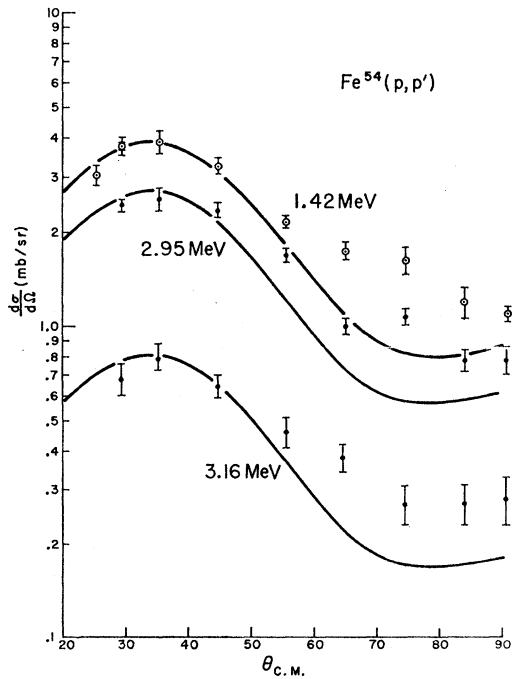


FIG. 5. Angular distributions for the inelastic scattering of protons from the 1.42, 2.95, and 3.16 MeV levels of Fe^{54} . The solid lines are $l=2$ DW curves.

The elastic peak is not shown. The oxygen and carbon content in the target was appreciable, and the elastic peaks can be seen at channels 328 and 338. The differential cross sections for inelastic scattering are shown in Figs. 5-7. The solid lines through the data points are DW fits normalized to the data. Since the shell-

TABLE II. Energy levels of Fe^{54} .

Aspinall <i>et al.</i> ^a (MeV)	This work (MeV)
1.408	1.42
2.540 ^b	2.53
2.563	...
2.961	2.95
3.161	3.16
3.291	3.28
3.340	...
3.829	3.82
4.029	...
4.047	4.05
4.070	...
4.265	4.26
4.287	...
4.579	...
4.656	...
4.700	...
4.781	4.76

^a See Ref. 23.

^b May be doublet.

model and collective-model DW cross section shapes are nearly identical, either model can be used for this purpose.

The energy levels of Fe^{54} listed in Table II were taken from the compilation of Way *et al.*²² and from the recent work of Aspinall, Brown, and Warren²³ who studied the inelastic scattering of 11.97-MeV protons. The levels excited by the inelastic scattering of 17.45-MeV protons are also listed in Table II for comparison. The 2.53-MeV levels seen in this work could be a mixture of the 2.540- and 2.563-MeV levels seen by Aspinall *et al.*²³ The levels at 4.05, 4.26, and 4.76 MeV are likely also to contain contributions from two or more levels.

A spin sequence of $6+$, $4+$, $2+$ for levels at 2.97, 2.55, and 1.41 MeV was suggested by a study of the β decay of the 1.5-min isomeric state of Co^{54} by Sutton, Hill, and Sherr.^{24,25} The angular distribution of the 1.42-MeV level in Fig. 5 supports the assignment of $2+$ to this level. The angular distribution of the 2.53-MeV level has the shape predicted for a $4+$ level and is also similar to the angular distribution of the known $4+$ levels in Cr^{52} at 2.37 and 2.77 MeV. While

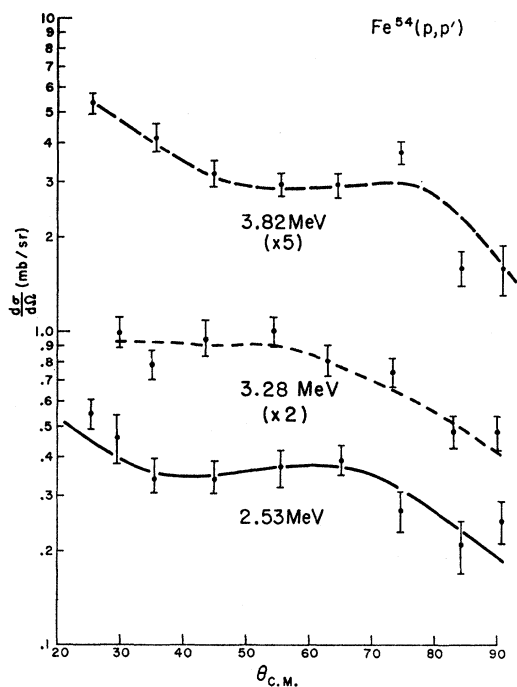


FIG. 6. Angular distributions for the inelastic scattering of protons from the 2.53-, 3.28-, and 3.82-MeV levels of Fe^{54} . The solid lines are $l=4$ DW curves; the dashed lines are lines drawn through the experimental points.

²² *Nuclear Data Sheets*, compiled by K. Way *et al.* (Printing and Publishing Office, National Academy of Science-National Research Council, Washington 25, D. C.), NRC 61-3-51.

²³ A. Aspinall, G. Brown, and S. E. Warren, *Nucl. Phys.* **46**, 33 (1963).

²⁴ D. C. Sutton, H. A. Hill, and R. Sherr, *Bull. Am. Phys. Soc.* **4**, 278 (1959).

²⁵ D. C. Sutton, Princeton University Ph.D. thesis, 1961 (unpublished).

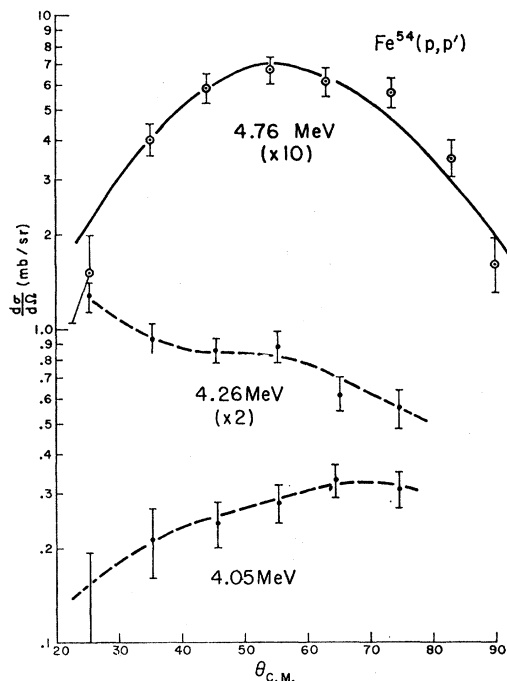


FIG. 7. Angular distributions for the inelastic scattering of protons from the 4.05-, 4.26-, and 4.76-MeV levels of Fe^{54} . The solid line is a $l=3$ DW curve.

this level may be double, an examination of the 72.5° spectra reported by Aspinall *et al.*²³ indicates that the major contribution is probably from the 2.540-MeV level. The 2.95-MeV level is definitely a $2+$ level with a rather large cross section, so it seems unlikely that this is the level observed by Sutton *et al.*²⁴

The level at 3.16 MeV in Fig. 5 also has an angular distribution similar to that of the known $2+$ levels. The level at 4.76 MeV has the expected shape of a $3-$ angular distribution. While the cross section is smaller than for the $3-$ levels in Cr^{52} and Ti^{50} (about 1.6 mb/sr at 55°), the DW fit seems good enough for an assignment of $3-$. A suggested level scheme for Fe^{54} and the extraction of nuclear structure parameters will be presented in Secs. V and VI.

B. Cr^{52}

An energy spectrum of protons scattered from Cr^{52} is shown in Fig. 8 for a laboratory angle of 80° . The elastic peak is not shown. The peaks at channel 347 and 357 are due to the 0.564- ($\frac{1}{2}-$) MeV level in Cr^{58} , and to the 0.79- ($2+$) MeV Cr^{50} level. The differential cross sections for the inelastic scattering are shown in Figs. 9-11 with the DW fits as solid lines. The energy levels of Cr^{52} tabulated in Table III are the results of inelastic proton scattering at 14.7 MeV by Matsuda,²⁶ the results of a study of the 5.7-day β decay of Mn^{52} by Wilson *et al.*,²⁷ and the results of the present experiment.

²⁶ K. Matsuda, *Nucl. Phys.* **33**, 536 (1962).

²⁷ R. R. Wilson, A. A. Bartlett, J. J. Kraushaar, J. D. McCullen, and R. A. Ristinen, *Phys. Rev.* **125**, 1655 (1962).

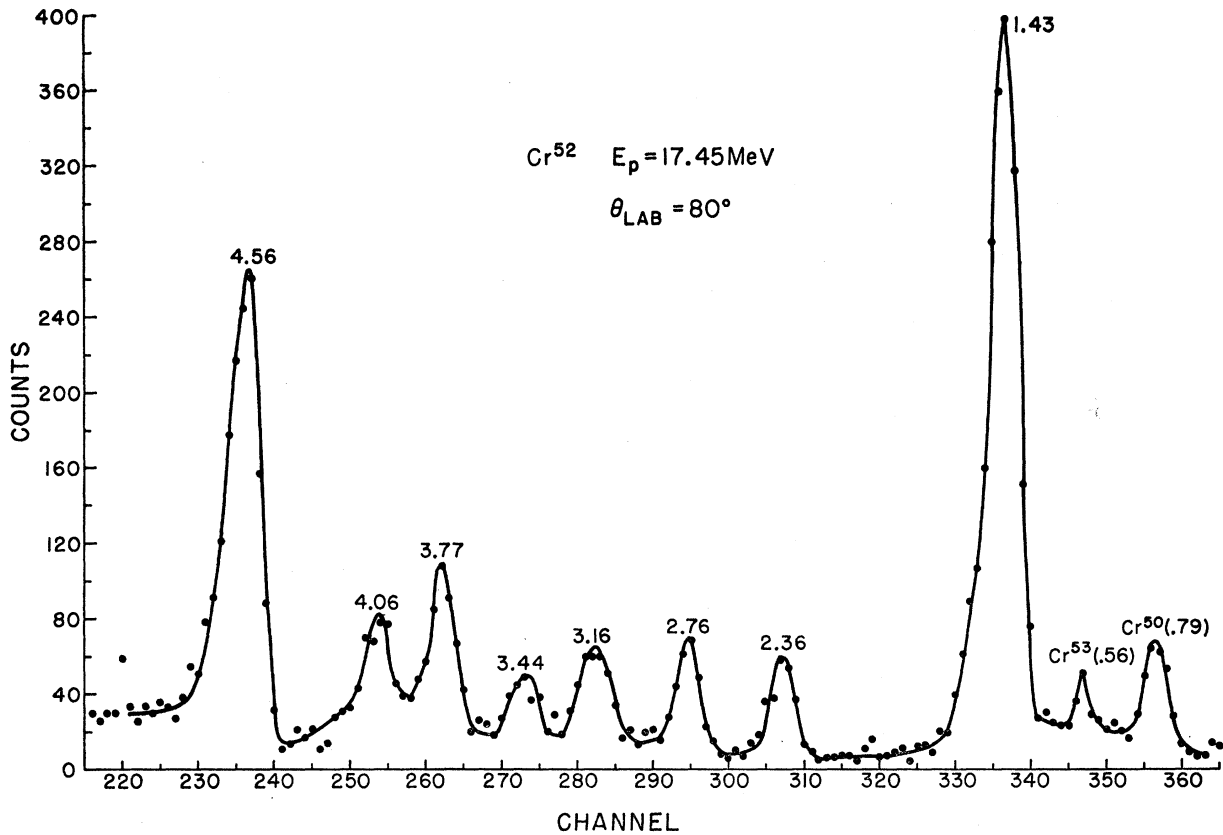


FIG. 8. Energy spectra of protons scattered from Cr^{52} . The curve is a smooth line drawn through the experimental points.

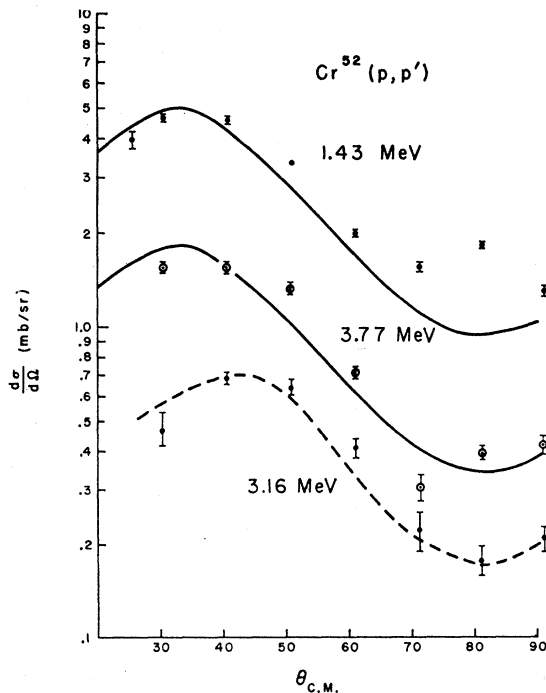


FIG. 9. Angular distributions for the inelastic scattering of protons from the 1.43-, 3.16-, and 3.77-MeV levels of Cr^{52} . The solid lines are $l=2$ DW curves.

The angular distributions of the 1.43- and 3.77-MeV levels shown in Fig. 9 support the spin assignment of $2+$ for these two levels. The 3.16-MeV level is also a probable $2+$ level. This is in agreement with Matsuda²⁶ who also suggested $2+$ for these levels. The known $4+$ levels at 2.36 and 2.76 MeV as shown in Fig. 10 agree with the DW analysis reasonably well. The analysis of the 4.56-MeV level shown in Fig. 11 confirms

TABLE III. Energy levels of Cr^{52} .

Matsuda ^a (MeV)	Wilson <i>et al.</i> ^b (MeV)	This work (MeV)
1.438	1.434	1.43
2.371	2.369	2.36
2.662	2.648	
2.768	2.766	2.76
2.963		
3.117	3.112	
3.162		3.16
3.432		3.44
3.494		
3.625	3.614	
3.767		3.77
3.926	3.832	
4.03		4.06
4.56		4.56

^a See Ref. 26.
^b See Ref. 27.

Matsuda's²⁶ assignment of $3-$. Crut *et al.*²⁸ observed a strong yield at 3.6 MeV using the (α, α') reaction and suggested that the spin of this level was $3-$. The results of this experiment indicate that they were probably observing the strong $2+$ level at 3.77 MeV. The angular distribution for the 3.44-MeV level was flat within the statistics with a cross section of about 0.15 mb/sr. The cross section for the 4.06-MeV level was less than 0.2 mb/sr at 70, 80, and 90°, the only angles for which it was observed.

An investigation of the β decay of 21-min Mn⁵² by Katoh *et al.*²⁹ revealed the following weak gamma rays, 0.70, 0.94, 1.02, 1.15, 1.37, and 1.52 MeV. The spin of the isomeric state is $2+$, and its decay should

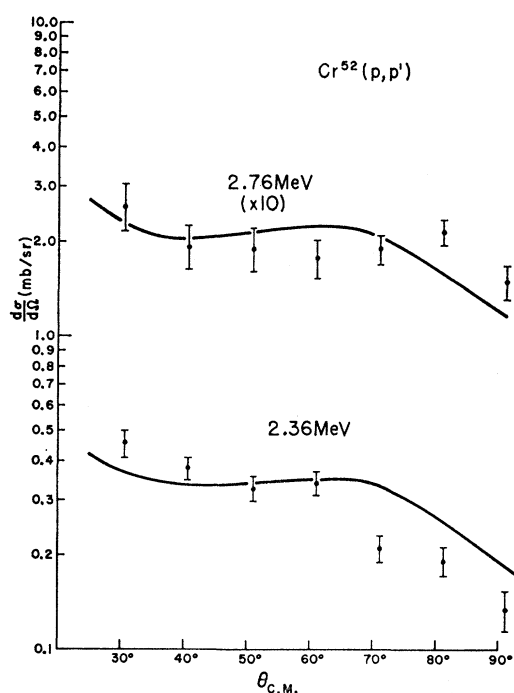


FIG. 10. Angular distributions for the inelastic scattering of protons from the 2.36- and 2.76-MeV levels of Cr⁵². The solid lines are $l=4$ DW curves.

involve low spin states of Cr⁵². Katoh *et al.* suggested a new level for Cr⁵² at 3.67 MeV to account for the 0.70- and 1.02-MeV gamma rays, but the data listed in Table III makes this level seem unlikely. The suggestion offered by Wilson *et al.*²⁷ that the 1.02- and 1.15-MeV gamma rays are transitions for a level at 3.80 MeV and that the 0.70-MeV radiation is from a level at 3.47 MeV is more acceptable. The 3.77- ($2+$) and the 3.44-MeV levels observed in this experiment are probably these levels. The excitation of the 3.44-MeV level was weak (<0.2 mb/sr) but the fact that it was observed argues for a low spin.

²⁸ M. Crut, D. R. Sweetman, and N. S. Wall, Nucl. Phys. **17**: 655 (1960).

²⁹ T. Katoh, M. Nozawa, Y. Yoshizawa, and Y. Koh, J. Phys. Soc. Japan **15**, 2140 (1960).

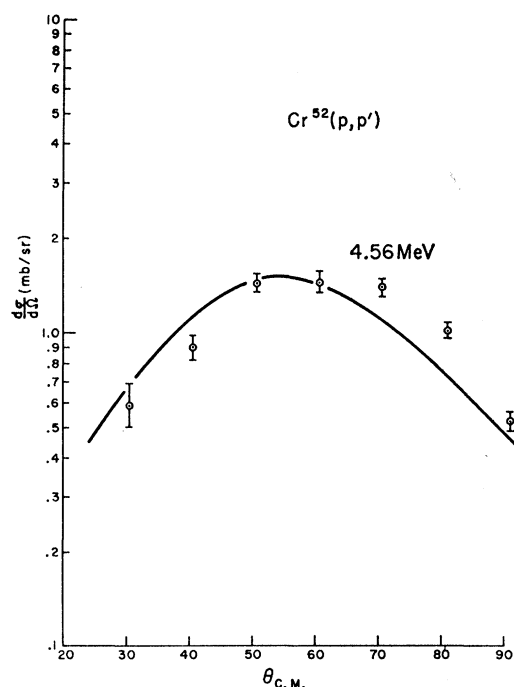


FIG. 11. Angular distribution for the inelastic scattering of protons from the 4.56-MeV level of Cr⁵². The solid line is the $l=3$ DW curve.

C. Ti⁵⁰

The energy spectrum of protons scattered from Ti⁵⁰ is shown in Fig. 12 for a laboratory angle of 60 deg. The elastic peak for Ti is not shown, but the elastic scattering from the contaminants oxygen and carbon is seen in channels 346 and 360.

The target contained 23% Ti⁴⁸ and a number of levels corresponding to known levels in Ti⁴⁸ were observed. To determine whether these levels did in fact belong to Ti⁴⁸, the energy spectrum of 17.5-MeV protons scattered from Ti⁴⁸ at 40° was taken. Table IV lists the levels

TABLE IV. Summary of energy levels observed with a Ti⁶⁰ target. The levels and cross sections observed at 40 degrees with a Ti⁴⁸ target are listed in columns 3 and 4, respectively. The relative cross sections of those levels from the Ti⁵⁰ target suspected of being Ti⁴⁸ levels are listed in column 5.

70% Ti ⁵⁰ This work	Ti ⁵⁰ Way <i>et al.</i> ^a	Ti ⁴⁸	Ti ⁴⁸ $\sigma(I)/\sigma(2+)$	Ti ⁵⁰ $\sigma(I)/\sigma(2+)$
0.98		0.98	1	1
1.55	1.570	2.31	0.10	
		2.42	0.13	
2.67	2.695	3.26	0.23	0.25
3.21	3.215	3.28	0.47	0.45
3.36		3.66	0.11	
		3.89	0.10	
		4.09	0.24	
4.14	4.14			0.70
4.38				
	4.88			

^a See Ref. 22.

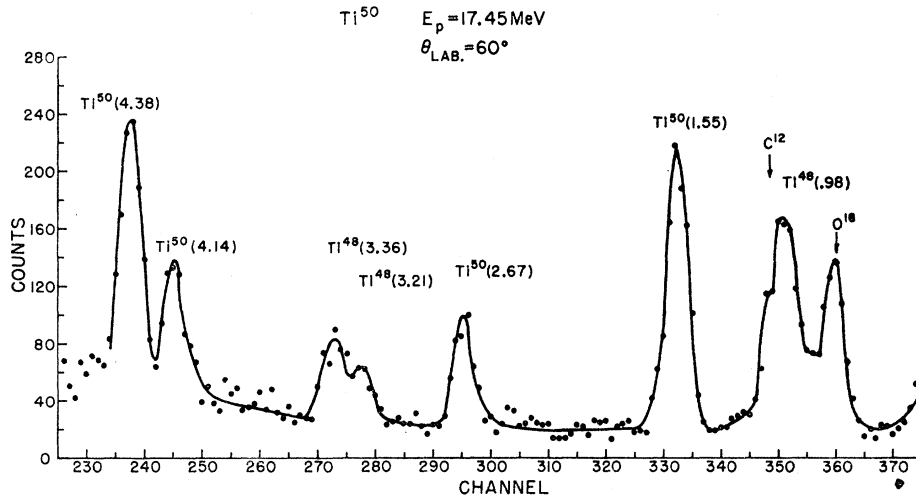


FIG. 12. Energy spectra of protons scattered from Ti^{50} .

observed with this target along with the known levels of Ti^{50} taken from the tabulation of Way *et al.*²² The energies of the first 2+, 4+, and 6+ levels of Ti^{50} have been changed to agree with the more recent work of Chilosi *et al.*,³⁰ who carried out a detailed investigation of the β decay of 1.7-min Sc^{50} , and observed the level sequence $0(0+)$, 1.570(2+), 2.695(4+), and 3.215(6+) MeV. The levels of Ti^{48} observed in the 40° spectrum are listed in column three, and the fourth column contains the differential cross sections relative to the

0.98- (2+) MeV level. The last column is the results from the Ti^{50} target. The levels at 0.98, 3.21, and 3.36 MeV are thus shown to be from the Ti^{48} in the Ti^{50} target. The 4.14-MeV level of Ti^{50} may have some contamination from the 4.09-MeV Ti^{48} level. However, since the cross sections were determined by fitting each peak with a standard curve derived from the ground-state peak, the contamination should be less than 15%.

The angular distributions for $Ti^{50}(p, p')$ are shown in Figs. 13 and 14. The DW analysis confirms the spin

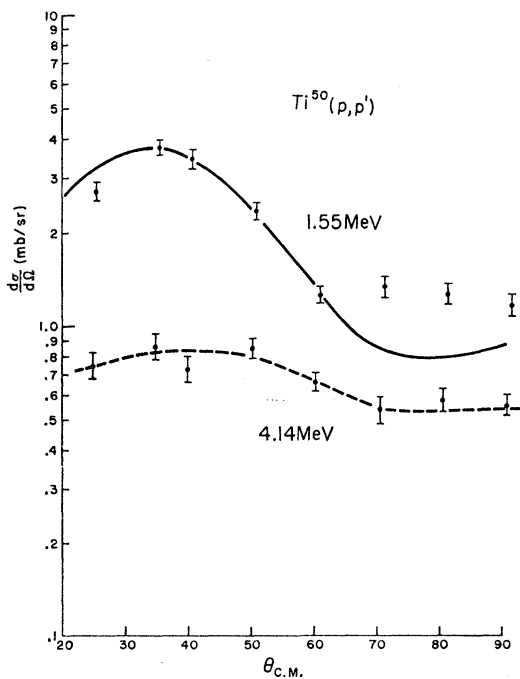


FIG. 13. Angular distributions for the inelastic scattering of protons from the 1.55- and 4.14-MeV levels of Ti^{50} . The solid line is the $l=2$ DW curve.

³⁰ G. Chilosi, P. Cuzzocrea, G. B. Vingiani, R. A. Ricci, and H. Morinaga, Nuovo Cimento 27, 86 (1963).

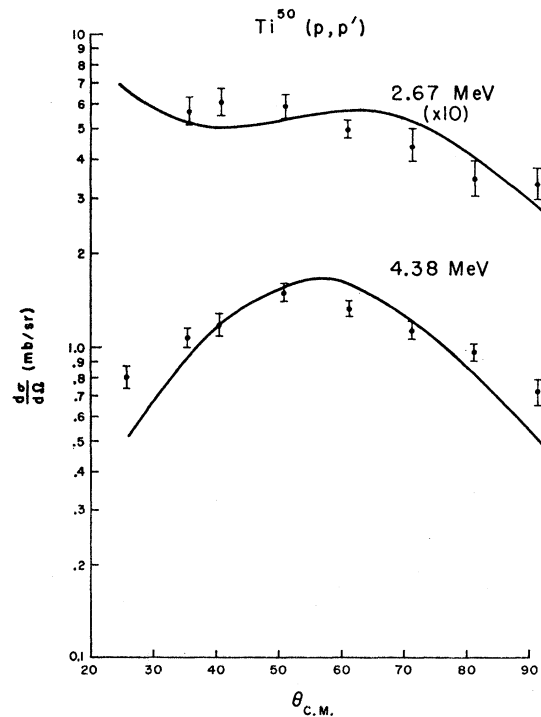


FIG. 14. Angular distributions for the inelastic scattering of protons from the 2.67- and 4.38-MeV levels of Ti^{50} . The solid lines are DW curves for $l=4$ and $l=3$, respectively.

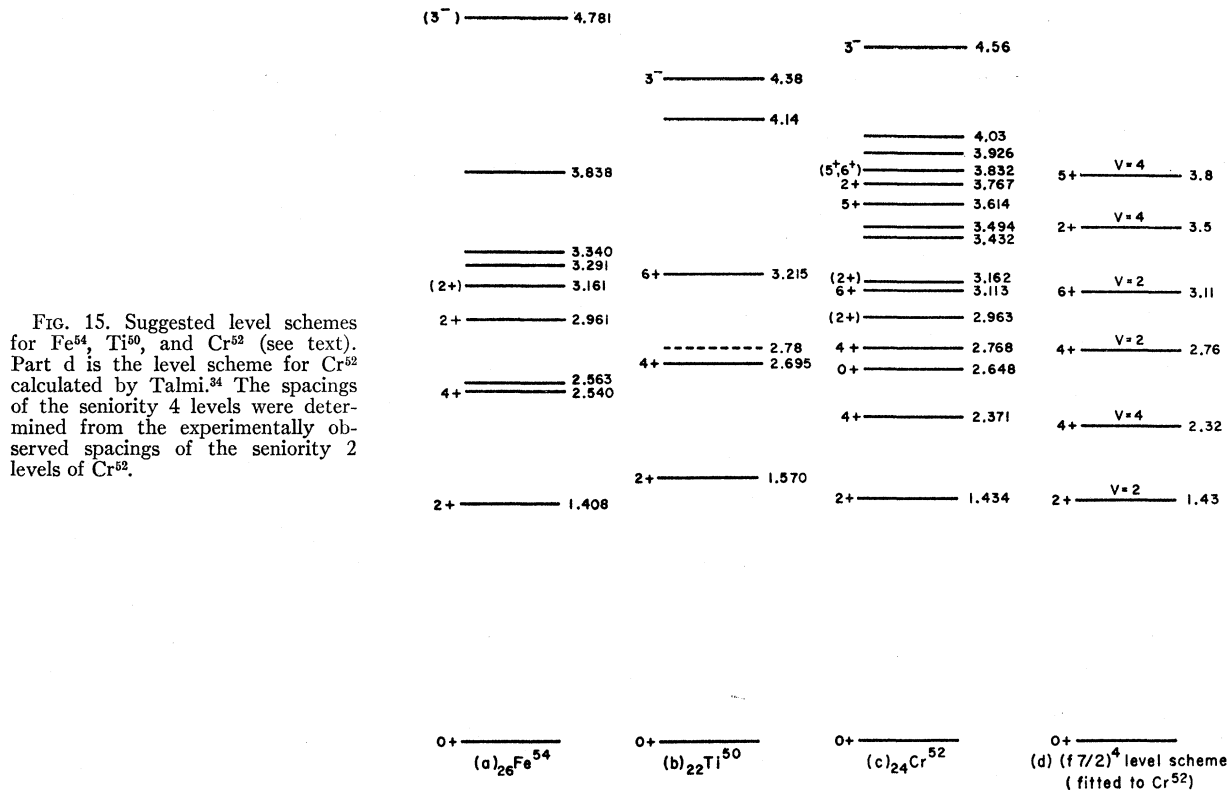


FIG. 15. Suggested level schemes for Fe^{54} , Ti^{50} , and Cr^{52} (see text). Part d is the level scheme for Cr^{52} calculated by Talmi.³⁴ The spacings of the seniority 4 levels were determined from the experimentally observed spacings of the seniority 2 levels of Cr^{52} .

assignment of 2+ and 4+ to the 1.55- and 2.67-MeV levels, and assigns a spin of 3- to the 4.38-MeV level.

V. DISCUSSION OF ENERGY LEVELS FOR THE EVEN-EVEN NUCLEI

Suggested level schemes for Fe^{54} , Ti^{50} , and Cr^{52} are shown in Fig. 15. The energies are taken from Way *et al.*,²² Aspinall *et al.*,²³ and Wilson *et al.*,²⁷ except for those levels determined in this experiment. The spins of the 3.61- and 2.65-MeV levels of Cr^{52} have recently been determined and are shown in Fig. 15 for completeness. Kaplan and Shirley³¹ have found a 5+ spin for the 3.61-MeV level by using a low-temperature nuclear orientation experiment. Finally, the level at 2.65 MeV has been assigned a spin 0+ in a preliminary report of a $(p, p'\gamma)$ angular correlation study by Kaye and Willmot.³² The interpretation of these level schemes in terms of nuclear models follows.

The energy levels of a $(f7/2)^n$ configuration will depend on the nature of the interparticle interaction. However, assuming only that the effective nuclear forces are two-body forces, the energy matrix elements in the $(f7/2)^n$ configuration are linear combinations of the matrix elements in the $(f7/2)^2$ configuration³³ and seniority is a good quantum number. Relationships thus

exist between energy levels in various configurations. In particular, the three nuclei studied here should have a 0+, 2+, 4+, and 6+ sequence of levels, in which the 2+, 4+, and 6+ levels have seniority 2 and have identical energy separations. de Shalit and Talmi³³ have examined this feature and in general the agreement is good. For Cr^{52} , there is also a sequence of 2+, 4+, 5+, and 8+ levels with seniority 4 whose spacing can be calculated from the experimental observed spacing of the seniority 2 levels. Talmi³⁴ has carried out such a calculation for Cr^{52} and his results are shown in Fig. 15d. The 4+ and 5+ seniority 4 levels agree well with the known 4+ level at 2.37 MeV and the 5+ level at 3.61 MeV.

Since inelastic proton scattering should not excite seniority 4 levels, the almost equal excitation of the 2.37- and 2.77-MeV levels implies that there is considerable seniority mixing for these two 4+ levels and therefore configuration mixing (assuming two-body forces). The same conclusion has been reached in an analysis of the $\text{Mn}^{55}(p, \alpha)\text{Cr}^{52}$ reaction by Sherr.³⁵

The seniority quantum number might be better for the 2+ levels since the energy separation is larger. Van Patter *et al.*,³⁶ using the $(n, n'\gamma)$ reaction, have

³⁴ I. Talmi, Phys. Rev. **126**, 1096 (1962).

³¹ M. Kaplan and D. A. Shirley, Nucl. Phys. **37**, 522 (1962).
³² G. Kaye and J. C. Willmott, Abstracts of the Conference on Low Energy Nuclear Physics, 1962 (unpublished), p. 13.

³³ A. de-Shalit and I. Talmi, *Nuclear Shell Theory* (Academic Press Inc., New York, 1963), p. 349.

³⁵ R. Sherr, in *Proceedings of the International Symposium on Direct Interactions and Nuclear Reaction Mechanisms, Padua* (Gordon and Breach, New York, 1963), p. 1025.

³⁶ D. M. Van Patter, N. Nath, S. M. Shafroth, S. S. Malik, and M. A. Rothman, Phys. Rev. **128**, 1246 (1962).

suggested a spin of 2+ for the 2.96-MeV level. Since this level is unexcited by the (p,p') reaction, an argument can be made for assigning seniority 4 to this level although the energy is somewhat lower than predicted. The classification of the 3.16- and 3.77-MeV levels is unclear.

Although the even-even nuclei under consideration here are below the "vibration" region³⁷ (which begins at $N \approx 32$), a vibration-model analysis may still be considered for Cr^{52} and Fe^{54} where second and third 2+ levels have been observed. Shakin and Kerman³⁸ describe the nucleus in terms of collective vibrations and by expanding the Hamiltonian to cubic terms predict deviations from the simple harmonic-oscillator spectrum. Expressions are given which describe the relative positions of the one-phonon (2+), two-phonon (0+, 2+, 4+) and three-phonon (0+, 2+, 3+, 4+, 6+) levels in terms of two parameters α and $(\beta')^2$.

Using the 1.41-, 2.54-, and 2.95-MeV levels of Fe^{54} as the one-phonon 2+, two phonon 4+, and two-phonon 2+ levels, respectively, the constants were determined: $\alpha = -0.13$ and $(\beta')^2 = 0.075$. The calculated positions of the two-phonon 0+ and the three-phonon 2+ are 1.85 and 3.13 MeV. The 2+ level is in agreement with the experimentally observed level at 3.16 MeV, but the occurrence of a 0+ level below the first 4+ level has not been observed. For Cr^{52} it was impossible to find the parameters α and $(\beta')^2$ if the two-phonon state was assumed to be the 3.16-MeV level. However, by assuming a two-phonon level at about 2.96 MeV, the three-phonon 2+ level was calculated to occur at 3.7 MeV and the two-phonon 0+ at 2.5 MeV. The parameters needed were $\alpha = -0.21$, and $(\beta')^2 = 0.024$, and the results seem to account for the 0+ (2.65) and 2+ (3.77) levels. The necessity of varying parameters by factors of 2 between Cr^{52} and Fe^{54} is not satisfactory.

Raz³⁹ has examined a system in which two identical $j = \frac{7}{2}$ particles are coupled to a core having collective surface excitation. The energy matrix was diagonalized for various values of the two-body interaction strength D and the surface interaction parameter χ . While this model applies specifically to Ti^{50} , it was applied also to Fe^{54} which has a $(f7/2)^{-2}$ configuration. The salient features of the data, namely, the absences of multiple-phonon levels below 6 MeV for Ti^{50} and the presence of a strongly excited second 2+ level near the first 6+ level for Fe^{54} , are correctly predicted. It was necessary, however, to increase the two-body interaction strength by a factor of 2 in going from Ti^{50} to Fe^{54} .

In view of the above, the importance of collective effects for the even-even $N = 28$ nuclei is not at all clear. The shell model still seems to be the best picture available for this region.

VI. DISCUSSION OF THE CROSS SECTIONS FOR THE EVEN-EVEN NUCLEI

The results of a DW analysis are shown in Table V. The energies and spins are listed in columns 2 and 3 with uncertain spins enclosed with brackets. The experimental differential cross sections in column 4 were taken at 35° for 2+, 65° for 4+, and 55° for 3- levels. The values of β_l determined from comparing theory to experiment are listed in column 5 of Table V. In all cases the value of β_l for the first 2+ states is about 0.15: for the 4+ states, ~ 0.10 , and for the 3- states, ~ 0.15 .

It is interesting to compare the values of β_2 obtained from inelastic scattering with those obtained by Coulomb excitation. Table VI presents this comparison and also presents results⁴⁰ for Ti^{48} , Fe^{56} , and Fe^{58} . Blair⁴¹ has suggested that the deformation distance $\beta_l R_0$ is the appropriate parameter with which to compare normalization constants from different theories, and therefore $\beta_2 R_0$ is tabulated in Table VI. Using the formula⁴²

TABLE V. Summary of results of the distorted-wave analysis. The experimental cross sections are listed for 35° (2+), 55° (3-), and 65° (4+). The normalization parameters of the collective-model and shell-model theories are denoted by β_l and V_G , respectively. The listed energies are the same as in Fig. 15 and may differ slightly from energies referred to in the text.

Isotope	Energy	Spin	$(d\sigma/d\Omega)_{\text{exp}}$	β_l	V_G
Ti^{50}	1.57	2+	3.7 mb/sr	0.15	45 MeV
	2.69	4+	0.52	0.11	60
	4.38	3-	1.6	0.17	
	1.43	2+	5.1	0.17	44
	2.37	4+	0.36	0.09	55
Cr^{52}	2.77	4+	0.20	0.07	
	3.16	(2+)	0.70		
	3.77	2+	1.7	0.11	
	4.56	3-	1.5	0.16	
	1.41	2+	3.7	0.14	45
Fe^{54}	2.54	4+	0.38	0.09	52
	2.96	2+	2.8	0.13	
	3.16	(2+)	0.70		
	4.78	(3-)	0.70	0.11	

TABLE VI. Comparison of $\beta_2 R_0$ as determined by inelastic proton scattering at 17.5 MeV and by Coulomb excitation. R_0 is in Fermis.

Isotope	$\beta_2 R_0(\text{inel.})$	$\beta_2 R_0(\text{Coul.})$	$\beta(\text{Coul.})$
			$\beta(\text{inel.})$
Ti^{48}	0.95	1.18	1.2
Ti^{50}	0.69		
Cr^{52}	0.70	0.98	1.2
Fe^{54}	0.71		
Fe^{56}	1.05	1.15	1.1
Fe^{58}	0.97	1.21	1.2

³⁷ G. Scharff-Goldhaber and J. Weneser, Phys. Rev. **98**, 212 (1955).

³⁸ A. K. Kerman and C. M. Shakin, Phys. Letters **1**, 151 (1962).

³⁹ B. J. Raz, Phys. Rev. **129**, 2622 (1963).

⁴⁰ H. O. Funsten and N. R. Roberson, Bull. Am. Phys. Soc. **8**, 367 (1963).

⁴¹ J. S. Blair (private communication).

⁴² A. Bohr and B. Mottelson, Kgl. Danske Videnskab. Selskab, Mat. Fys. Medd. **27**, No. 16 (1953).

for a uniformly charged spheroid

$$B(El) = [(3/4\pi)e^2ZR^l]^2[\beta_l^2/(2l+1)]. \quad (16)$$

the $\beta_2(EM)$'s were calculated from the experimental $B(E2)$'s as determined from Coulomb excitation studies by Gove and Broude⁴³ and Lemburg.⁴⁴ The ratio of the $\beta_2(EM)$ to $\beta_2(\text{inel})$ is given in the last column of Table VI and is rather constant with a value of about 1.15. The close agreement between the β_2R_0 values extracted from (p,p') and those extracted from Coulomb excitation is striking. These values compare very well with values extracted from the (α,α') reaction by similar techniques.⁴⁵

The inelastic scattering from 4+ levels is not well understood at present. Beurtey *et al.*⁴⁶ have observed that the Blair phase rule³ is violated for the inelastic scattering of alpha particles from the lowest lying 4+ level of Fe⁵⁶ and Ni⁵⁸. These levels are suggested to be part of the two-phonon triplet of the quadruple vibrational states of these nuclei. Austern *et al.*⁴⁷ have investigated these "anomalous-phase" angular distributions and have shown that terms representing simultaneous and successive excitation of two phonons are both important in the DW analysis and, moreover, that agreement with experiment is obtained only because of cancellation between these terms. The DW curves used to fit the present data were calculated not assuming a two-phonon excitation, but rather assuming that the states are described as a single 2⁴-pole deformation or vibration. The $l=4$ DW curves in Figs. 2 and 3 demonstrate that the shape of the angular distribution is not sensitive to the form factor. Until the 4+ levels are better understood, the experimental deformation parameters β_4 should be considered only as a convenient way to characterize the data.

The theoretical curves used to fit the 3- angular distribution were calculated assuming an octupole deformation or vibration, and are in good agreement with the experiment. The extracted β_3 values are listed in Table V. The $B(E3)$ for the 3.73 MeV of Ca⁴⁰ has been measured by Helm⁴⁸ and a value $\beta_3=0.3$ was obtained using Eq. (16). The use of a uniform charge distribution here is very questionable, since β_3 depends on R^6 . An analysis of 43-MeV inelastic alpha scattering from Ni⁵⁸ gave $\beta_3=0.14$ for the 3- level.⁴⁵ Thus, the magnitudes of the β_3 values extracted from the present

data are comparable to those available for other 3- levels in this mass region.

The β_2 values for the other strongly excited 2+ states are also listed in Table V. If these second and third 2+ levels are due to collective vibrations of the nuclear surface, then the collective model used is incorrect, since terms of the order of β^2 must also be included in the expansion of the interaction potential. As with β_4 , these β_2 values do serve as a convenient number with which to characterize the experimental angular distribution.

The shell-model DW theory may also be applied to the analysis of Ti⁵⁰, Cr⁵², and Fe⁵⁴. Using the values of the reduced matrix elements listed in Table I, the strength parameter V_G was determined from the data and is listed in column 6 of Table V. For the 2+ levels, the relative agreement is very good. The experimental cross sections were equal for Ti⁵⁰ and Fe⁵⁴ as expected from the shell model, and the increase for Cr⁵² is that predicted by the reduced matrix element. The value of $V_G=45$ MeV which is extracted appears to be comparable with two-body well depths. However, the interaction used was assumed to be of Wigner-exchange form and thus would not fit two-body scattering data well. If one assumes a Serber-exchange mixture and ignores all exchange integrals, the strength parameter V_G should be multiplied by a factor 8/3.^{48a} The resulting strength is then in agreement with that found by Levinson and Banerjee⁴⁹ for the C¹² (p,p') C^{12*} (4.43) reaction and is also consistent with the large (~ 6) collective enhancements of electromagnetic transition probabilities.⁵⁰

VII. INELASTIC SCATTERING FROM V⁵¹

As was seen in Sec. VI, the inelastic scattering from the first 2+ level of the even-even nuclei with 28 neutrons could be adequately described from either the shell model or the collective model point of view. Odd- A nuclei, however, require a more detailed description. A very reasonable collective model for V⁵¹ is the weak-coupling model. In this model, the low-lying excited states of V⁵¹ are described by a single proton ($j=7/2$) coupled to a Ti⁵⁰, 2+ vibrational "core." This yields a 3/2, 5/2, 7/2, 9/2, and 11/2 multiplet of levels. The inelastic scattering to any of these levels has a $l=2$ angular distribution with the intensity obeying

$$\left(\frac{d\sigma}{d\Omega}\right)_{I_f} = \frac{2I_f+1}{(2I_i+1)(2I_c+1)} \left(\frac{d\sigma}{d\Omega}\right)_{I_c}, \quad (18)$$

where I_i , I_f , and I_c are the ground state, excited state and "core" spin, respectively. Also the sum of all the multiplet cross sections should equal the Ti⁵⁰ (p,p') Ti^{50*} (2+) inelastic cross section.

^{48a} We are grateful to Dr. G. R. Satchler for pointing out this fact.

⁴⁹ C. A. Levinson and M. K. Banerjee, *Ann. Phys. (N. Y.)* **3**, 67 (1958).

⁴⁷ N. Austern, R. M. Drisko, E. Rost, and G. R. Satchler, *Phys. Rev.* **128**, 733 (1962).

⁴⁸ R. H. Helm, *Phys. Rev.* **104**, 1466 (1956).

⁵⁰ H. W. Kendall and I. Talmi, *Phys. Rev.* **128**, 792 (1962).

⁴³ H. E. Gove and C. Broude, in *Proceedings of the Second Conference on Reactions between Complex Nuclei, 1960*, edited by A. Zucher, E. C. Halbert, and F. T. Howard (John Wiley & Sons, Inc., 1960), p. 57.

⁴⁴ I. Kh. Lemburg, in *Proceedings of the Second Conference on Reactions between Complex Nuclei, 1960*, edited by A. Zucher, E. C. Halbert, and F. T. Howard (John Wiley & Sons, Inc., New York, 1960), p. 112.

⁴⁵ E. Rost, *Phys. Rev.* **128**, 2708 (1962).

⁴⁶ M. Beurtey, P. Catillon, R. Chaminade, M. Crut, H. Faraggi, A. Papineau, J. Sandinos, and J. Thirion, *Compt. Rend.* **252**, 1758 (1961).

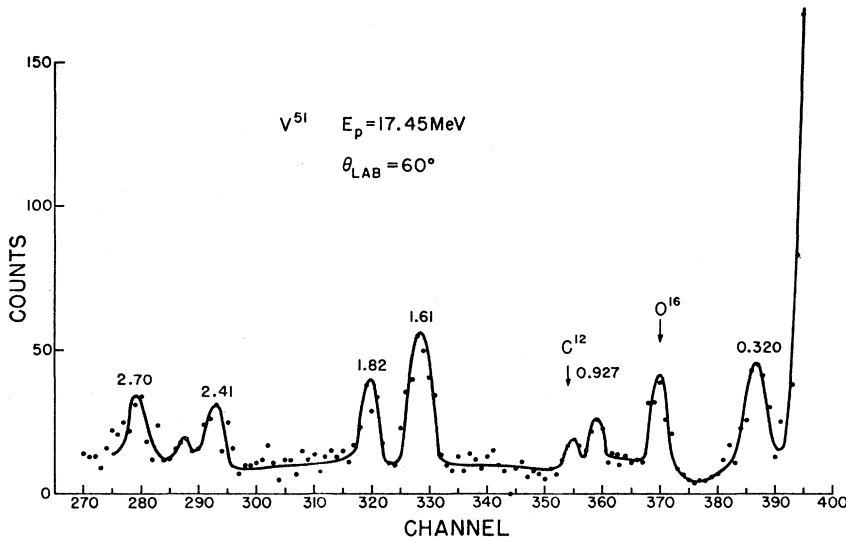


FIG. 16. Energy spectra of protons scattered from V^{51} .

The weak-coupling model has been successful in explaining the $Cu^{63}(p,p')Cu^{63*}$ reaction.⁵¹ The sum rule prediction has been tested with high-energy electrons⁵² and found to hold for Co^{59} . Kendall and Talmi⁵⁰ have studied the inelastic electron scattering by V^{51} , but

their data did not distinguish between the weak-coupling model or the usual shell model. It is therefore of interest to use both models to study the structure of V^{51} .

An energy spectrum of protons scattered from V^{51} for a laboratory scattering angle of 60° is shown in Fig. 16. The rise in counts for channels above 390 is the low-energy side of the elastic scattering peak for V^{51} . Elastic

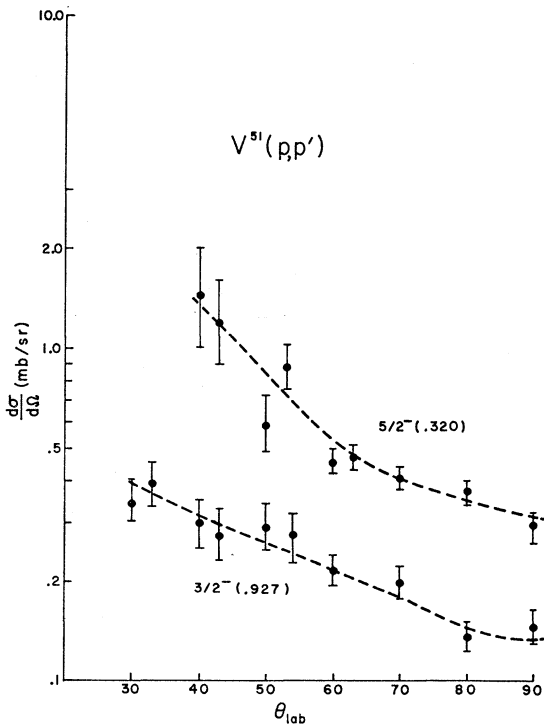


FIG. 17. Angular distributions for the inelastic scattering of protons from the 0.320- and 0.927-MeV levels of V^{51} . The dashed lines are just curves drawn through the experimental points.

⁵¹ F. Perey, R. J. Silva, and G. R. Satchler, Phys. Letters 4, 25 (1963).

⁵² H. Crannell, R. Helm, H. Kendall, J. Oeser, and M. Yearian, Phys. Rev. 123, 923 (1961).

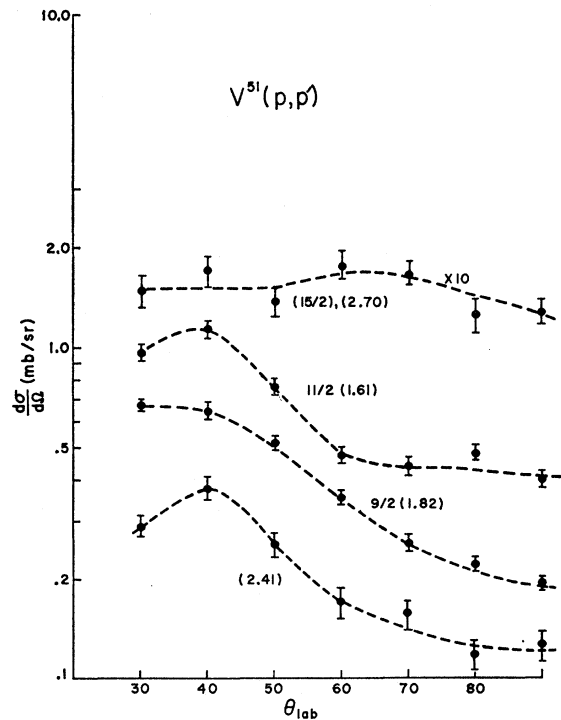


FIG. 18. Angular distributions for the inelastic scattering of protons from the 1.82-, 1.61-, 2.41-, and 2.70-MeV levels of V^{51} . The dashed lines are curves drawn through the experimental points.

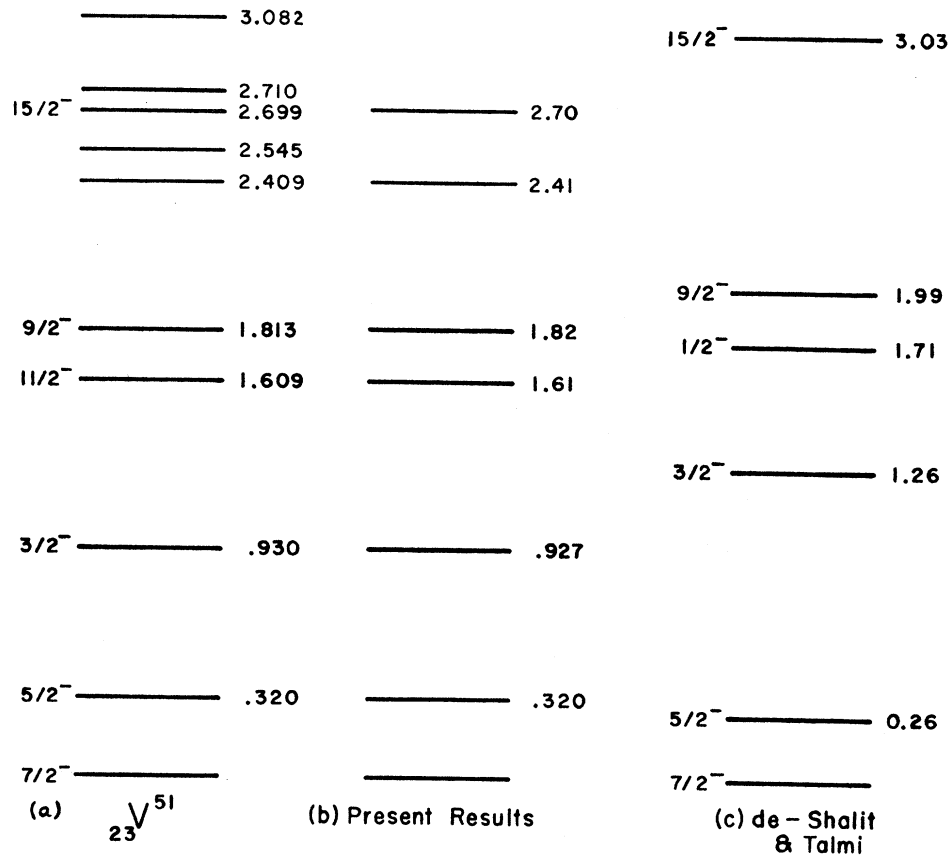


FIG. 19. (a) The level scheme of V^{51} taken from Schwager (Ref. 53). (b) The levels observed in this work. (c) The calculated energy levels of V^{51} as determined from the spacing of the seniority 2 levels of Ti^{50} , Cr^{52} , and Fe^{54} .

peaks from O^{16} and C^{12} are also seen. The cross section for the first-excited state at 0.32 MeV was obtained for all angles except 30° where the elastic scattering predominates. The angular distributions are given in Figs. 17 and 18. The dashed curves are smooth lines drawn through the experimental points.

The energy levels of V^{51} are shown in Fig. 19(a) and were taken from the article by Schwager.⁵³ Figure 19(b) shows the result of the present experiment. A small peak is seen at channel 288 in Fig. 16 which corresponds to the known level at 2.54 MeV, but because this level was not seen at other angles it is not shown in Fig. 19(b). The energy levels shown in Fig. 19(c) are calculated with a shell-model formalism using the experimentally measured splitting of the $(f7/2)^2$ configuration.³³

Kendall and Talmi⁵⁰ have pointed out that the V^{51} level spectrum (the $I=7/2$ ground state, and the $I=5/2$, $3/2$, $11/2$, and $9/2$ excited states) cannot be explained by the weak coupling of the odd proton to a $2+$ core state since the energy spread of these levels is as large as the $I=0$ to $I=2$ energy separation in Ti^{50} .

Also there is no known $7/2^-$ excited state. It is interesting, however, that by assuming the 2.41-MeV level has spin $7/2^-$, the center of gravity of the multiplet is 1.56 MeV which is in good agreement with the 1.55-MeV $2+$ state in Ti^{50} or the 1.43-MeV $2+$ state in Cr^{52} .

None of the angular distributions shown in Figs. 17 and 18 is well described by a pure $l=2$ DW curve. Nevertheless, distorted-wave $l=2$ angular distributions were fitted to the $3/2$, $5/2$, $9/2$, and $11/2$ levels and the cross sections at 35° were determined. These are shown in Table VII relative to the $3/2^-$ level along with the relative cross section based on the weak-coupling model

TABLE VII. Comparison of experiment to the weak-coupling model. The table gives the cross sections for each level measured at 35° (see text) and the cross section relative to the $3/2$ level, R_{exp} . R_{th} is the prediction of the weak-coupling model.

Level	$d\sigma/d\Omega$	R_{exp}	R_{th}
$3/2$	0.4	1.0	1.0
$5/2$	1.5	3.8	1.5
$9/2$	0.6	1.5	2.5
$11/2$	1.1	2.8	3.0

⁵³ J. E. Schwager, Phys. Rev. **121**, 569 (1961). This article contains a large number of references on the shell-model calculations of V^{51} .

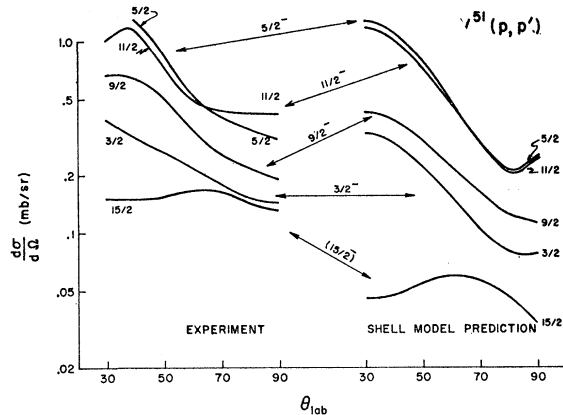


FIG. 20. Comparison of the experimental cross sections of V^{51} with the theoretical predictions based on the shell model (see text). The experimental data are smooth curves drawn through the experimental points.

prediction. Thus, both the $l=2$ angular distribution requirement and the intensity rule are violated.⁵⁴

The shell-model theory has been presented in Sec. III and is given by a weighted sum of the $l=2, 4,$ and 6 angular distributions of Fig. 3. Using the angular matrix elements in Table I and a value $V_G=45$ MeV, one obtained the differential cross sections which are presented in Fig. 20 along with the experimental results. The solid lines shown for the experimental data are smooth curves drawn through the data. It should be noted that the strength parameter, V_G , has the same value as it does in the analysis of Ti^{50} , Cr^{52} , and Fe^{54} and that no further parameters are left in the theory.

The agreement is rather good in that the correct ordering of the levels is predicted as well as the magnitudes of the excitations. Only the $15/2$ level is in disagreement and this level differs from the others in having no $l=2$ component. However, it should be noted that the spin assignment for this level is less certain than for the $3/2, 5/2, 9/2,$ and $11/2$ levels.

⁵⁴ The intensity rule would be satisfied if the spins of the first four excited states were $11/2, 3/2, 9/2, 5/2$.

SUMMARY AND CONCLUSION

The major points of the (p, p') results at $E_p=17.45$ MeV can be summarized as follows:

1. The analysis of the first $2+$ levels of even-even nuclei using the distorted-wave theory based on the collective model yields quadrupole deformation parameters which are in reasonable agreement with those obtained by Coulomb excitation.

2. The same levels have also been studied with a distorted-wave analysis based on the shell model. Assuming that only the protons in $(f7/2)^n$ configurations take part in the (p, p') reaction, a constant value of 45 MeV was obtained for the strength parameter. Thus, the analysis does not distinguish between the shell model or collective model.

3. The observation of second and third $2+$ states in Cr^{52} and Fe^{54} suggests that a vibrational model may explain the highly excited states of these nuclei. These $2+$ levels may provide a sensitive test of nuclear models used in energy level calculations.

4. Strongly excited $3-$ levels were observed in the even-even nuclei and their angular distributions were correctly described by a DW analysis which assumed that these states are formed by an octupole surface deformation or vibration.

5. The results of the inelastic scattering from V^{51} were more sensitive to model. It was found that both the spin intensity rule and the angular-momentum transfer rule of the weak-coupling model were not valid for V^{51} . However, assuming a $(f7/2)^3$ configuration for the protons in V^{51} and a value of $V_G=45$ MeV, the DW theory based on the shell model was in good agreement with the data.

ACKNOWLEDGMENTS

We wish to thank Professor R. Sherr and Professor B. Bayman for many valuable discussions.